Stress profile in a two-dimensional silo: Effects induced by friction mobilization

Francisco Vivanco,[1,*] José Mercado,[1] Francisco Santibáñez,[2] and Francisco Melo[1,†]
[1]*Laboratorio de Física no Lineal, Departamento de Física, Universidad de Santiago de Chile, Avenida Ecuador 3493, Casilla 307 correo 2, Santiago, Chile*
[2]*Instituto de Física, Pontificia Universidad Católica de Valparaíso, Avenida Brasil 2950, Valparaíso, Chile*
(Received 30 October 2015; revised manuscript received 17 May 2016; published 22 August 2016)

The effects of friction mobilization on the stress profile within a two-dimensional silo are investigated via simulations of discrete elements. Friction mobilization is driven by cyclic vertical displacement of the sidewalls. Two regimes have been observed for small filling height, with stress profiles identified as saturated (Janssen's profile) and exponentially growing. The transition between these regimes is denoted by an almost linear stress profile, similar to that of a hydrostatic system, with a significantly greater characteristic height compared to the height of the column of grains. For tall columns, the process of friction inversion is more complex. A partial inversion of friction mobilization is observed when the motion is reversed from upward to downward, which results in two coexisting zones of opposite mobilization. These zones are separated by a wide compaction front with a gradual upward progression sustained by the displacement of the walls. Conversely, if the motion is reversed, the two opposing friction mobilization zones retract, the transition zone becomes smooth, and the system rapidly transforms from two coexisting mobilization states to a Janssen-like regime. In both regimes, the general characteristics from the resulting stress profiles are depicted by generalizing Janssen's equation to include partial mobilization through the varying effective friction coefficient along the silo walls.

DOI: 10.1103/PhysRevE.94.022906

I. INTRODUCTION

Understanding the features of stress distribution in granular columns is a long-standing problem for the scientific community. Thus far it has been established that, depending on the preparation, in confined granular materials subjected to compaction, the pressure at the base of the column becomes saturated as the filling height increases. As a consequence, the stress distribution as a function of the vertical coordinate presents two well-defined regions: a hydrostatic region where the penetration from the free surface is a function of friction and preparation conditions, and a region where the stresses are nearly independent of the vertical coordinate. To describe this effect, Janssen [1] treated granular material as a continuous medium where vertical stresses σ_{zz} are deflected into horizontal stresses σ_{xx}, which is accounted for by a phenomenological law, $\sigma_{xx} = \kappa\sigma_{zz}$, where κ is a constant. Further to this assumption, Janssen assumed that the force of friction between particles and walls is described by the Coulomb failure criterion: $F_S = \mu F_N$, where F_S is the magnitude of the tangential friction force, F_N is the normal force at the wall, and μ is the coefficient of friction for particle-wall contacts. This assumption is also known as incipient failure or as a fully mobilized friction condition. In a two-dimensional silo of width D, filled to a height of z_0, considering the assumption that friction is fully mobilized in the opposite direction to the direction of gravity, Janssen's analysis predicts that the equilibrium equation is given by

$$-\frac{d\sigma_{zz}}{dz} + \frac{\kappa\mu}{D}\sigma_{zz} = \rho g\phi, \tag{1}$$

where ϕ is the granular packing fraction, ρ is the density of bulk material, and g the acceleration of gravity. With the condition $\sigma_{zz}(z_0) = 0$, this equation provides the vertical stress $\sigma_{zz}(z)$ at a height z,

$$\sigma_{zz}(z) = \rho g\phi l\left[1 - \exp\left(-\frac{z_0 - z}{l}\right)\right], \tag{2}$$

where $l = D/\kappa\mu$ is the screening length which determines the hydrostatic region. Notice that this stress exponentially converges to the value $\phi\rho gl$. The σ_{zz}, obtained from (2), is known as the Janssen profile.

However, it is very restrictive to assume the fulfillment of the fully mobilized friction hypothesis, since it is possible to obtain the force equilibrium at the silo walls for any shear force value $\sigma_{xz} < \mu\sigma_{xx}$, from which a family of solutions will arise. The fact there is a variety of solutions suggests that the wall force and packing are highly sensitive to the preparation conditions and the slight variations of the sidewalls. This sensitivity is partly due to the minimal sliding distance required to activate the friction force between two solid surfaces, which is related to the size of the asperities, 1 μm for typical surfaces, which is extremely small relative to other relevant distances. Early work of Evesque and de Gennes [2] provided evidence on the friction mobilization process during the filling of silos. By considering the granular packing as a continuous elastic material, it was proven that material displacement at the walls, due to the force of its own weight, was enough to fully mobilize friction forces in the walls, except at both ends of the silo.

Recent studies have cast doubt upon Janssen's concept, which was based on quasielasticity (elliptical equations). Modern techniques propose hyperbolic type equations, which are based on local and history-dependent relations between stress tensor components [3]. In general, both models predict similar features; however, notable differences may occur when an additional charge is added to the free surface of the silo [3].

*francisco.vivanco@usach.cl
†francisco.melo@usach.cl

Further work has shown that the additional charge is responsible for a nonmonotonic stress distribution, which presents a robust test for any theoretical model describing the statics under various loading histories and boundary conditions [4]. To our knowledge, interpretation of the mobilization history of frictional forces is still an unresolved issue, which is independent of the approach.

The variation in speed of vertical wall motion has been used to explore stress configurations [5]. Under these conditions, the apparent mass measurement at the base of the granular column demonstrated that Janssen's model is valid independently of the wall velocity. This was confirmed over a broad range of velocities. However, for grain columns of large heights, the limit of the apparent mass value is lower than its static value. This is likely to be due to a creep effect which occurs once motion ceases in the walls.

Furthermore, studies have been carried related to how the motion of the sidewall affects confined granular packing by discrete elements and molecular dynamic simulations, and the evolution of stress as a function of wall movement, in both a parallel and opposing motion relative to gravity, has been investigated [6]. However, to our knowledge, both the process of inverting friction mobilization through the reversing sidewall motion and the corresponding effects on stress profiles have not been addressed.

This article utilizes discrete element simulations to investigate how the stress profile is affected by the vertical displacement of sidewalls, in a two-dimensional silo. The upward motion of the sidewall causes a saturating stress profile, resembling Janssen's regime. In turn, reversing the motion—upward to downward—induces an inversion of the friction mobilization, modifying the stress profile from saturating to exponentially growing. This transition spans an interval of the displacement of the sidewall about a fraction of the particles' diameter, and is marked by a strong peak in the characteristic length of the stress profile, which indicates a hydrostatic stress profile during transition. When the sidewall motion is inverted—downward to upward—a similar behavior occurs: there is a near exponential increase, and then decrease of the characteristic length with wall displacement. However, for tall columns, the previous description is not entirely accurate, as portions of opposite friction mobilization are apparent. These regions of opposite friction mobilization are separated by a zone which progresses with the displacement of the sidewall. We show that this progression is strongly linked to a compaction or decompaction front, depending on whether the sidewalls are moving downward or upward. After a few cycles, a stationary regime is reached, in which compaction and decompaction are dominated by the elasticity of the contact network and do not involve significant plastic rearrangement of the network.

II. SIMULATION METHOD

We present discrete element method simulations (DEM) of a two-dimensional column of grains contained in a rectangular silo of $H \sim 2.1$ m height and $D \sim 0.125$ m width. The friction force on the walls is mobilized through the vertical movement of the silo sidewalls while maintaining the base fixed at $z = 0$ [Fig. 1(a)]. The silo is filled with a binary mixture

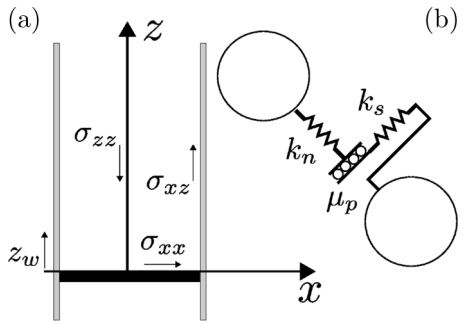

FIG. 1. (a) Schematic of stress components and coordinate system. z_w is the relative displacement between the sidewalls and the base, fixed at $z = 0$. (b) Scheme for the model of linear compression and Mohr-Coulomb plasticity without cohesion. k_n and k_s are normal and shear stiffness and μ_p is the friction coefficient of particles.

of disks with diameters of 8 mm (75%) and 9 mm (25%), which minimizes local crystallization. Two filling heights are investigated in detail, $h \sim 0.4$ m and $h \sim 1.2$ m, attained with $N = 700$ and $N = 2200$ particles, respectively. The corresponding aspect ratios, defined by the filling height ratio to the silo width, $R_a \equiv h/D$, are $R_a \sim 3.2$ and $R_a \sim 9.6$. The particles are characterized by their density $\rho_p \simeq 1130$ Kg/m^3, friction coefficient $\mu_p \simeq 0.8$, Young's modulus $E_p \simeq 4$ MPa, and Poisson's ratio $\nu_p \simeq 0.5$. Analogously, the characteristics of the sidewalls are $\rho \simeq 8000$ Kg/m^3, $\mu \simeq 0.8$, $E \sim 210$ GPa, and $\nu \simeq 0.5$. The particle characteristics are selected according to similarity to the softest photoelastic material that is commercially available, which permits the detection of forces in the order of the weight of a single grain. This material will be utilized in future experiments, under the same conditions of the simulation, for a direct comparison of results. The interactions between particles, and between particles and walls, are based on a model combining linear compression and Mohr-Coulomb plasticity without cohesion implemented in YADE [7–9] [Fig. 1(b)]. This model consists of three elements: the normal force $F_n = \min\{k_n u_n, 0\}$, the shear force $F_s = k_s u_s$, and the Mohr-Coulomb failure criterion $F_s^{\max} = \mu_p F_n$, where u_n and u_s are the corresponding normal and tangential displacements, μ_p the friction coefficient, and k_n and k_s the normal and shear stiffness constants, which are connected to the elastic properties of particles through $k_n = E_p d \sim 3.6$ kN/m and $k_s = \nu_p k_n \sim 1.8$ kN/m. Simulations are performed in two stages: the initial configuration, then the mobilization of the friction force. The initial configurations are prepared by distributing the particles over the entire silo, so at the outset they are distributed to form a random loose packing configuration. Initially, there should be a sufficient distance between particles to prevent overlapping and to preserve the initial packing once the grains are dropped. This preparation gives a packing fraction of $\phi \sim 0.76$, which is similar to the random loose packing value. Note that sidewalls remain fixed in their initial position during the preparation of the initial configurations. Subsequently, friction is mobilized at $t = 0$, by moving sidewalls downward and then upward at a constant speed ~ 9 mm/s, following a triangular wave of amplitude 9 mm over 10 periods. This procedure is repeated at least 20 times to generate different configurations, which present

a similar trend in the packing curve and stationary regime value. We verified that if the wall speed is kept low, i.e., in the quasistatic regime, where no inertial effect is involved, the stress distribution depends solely on the displacement of the sidewalls relative to the base. Due to the strong effect of the displacement amplitude of the sidewalls on friction mobilization, significant friction mobilization may occur even at small amplitude values. In order to ensure total mobilization, the amplitude of sidewalls' motion is chosen of the order of the diameter of larger particles. The effects on the vertical stress profile due to the friction mobilization on the sidewalls depend on the filling height, as shown in following results. It is important to mention that our two-dimensional (2D) simulations are limited with regards to the transposition of the results to 3D systems. Some of the limitations are related to the proclivity of 2D systems to crystallize, which is minimized by using a binary mixture of particles, and to reduce the particles mobility in the 2D system compared to the 3D system. For example, the extra degree of freedom in the latter decreases the effects due to the packing [10]. However, despite some of the features found in this system also being observed in 3D systems [11], these have not been systematically studied.

III. RESULTS

The variation over time of the total normal and shear forces on the sidewalls and base of the silo, F_N^W and F_S^W respectively, are shown in Figs. 2(a)–2(f). A gradual increase in F_N^W was observed, followed by a sudden relative decrease, with the maximum force occurring where the sidewalls' velocity is reversed [Fig. 2(a)–2(c) and 2(h) for wall motion]. Following several cycles, normal forces F_N^W tend to reach a stationary state, i.e., the behavior of the system is repeated from one cycle to the next, with the exception of some fluctuations. Loading and unloading are approximately linear with the displacement of the sidewalls; however, they occur at markedly different rates. The normal force at the base of the container presents the same features as observed at the sidewalls. All forces are in phase. Shear forces, F_S^W, exhibit a similar behavior, although, due to the choice of coordinates, the sign is opposite to that of normal forces. It should be noted that loading/unloading processes, observed in all force curves, are followed by force plateaus. As shown below, during these plateaus, friction in the wall is fully mobilized and therefore the system is in Janssen's state. However, it is apparent that the ratio of the shear force to the normal force outside plateaus, which is $F_S^W/F_N^W \sim 0.35 < \mu_p$, indicates that the friction force at the wall is not entirely mobilized during this part of the cycle. Conversely, and as expected, the shear force at the base [Fig. 2(f)] remains minimal, with exceptions occurring when the shear forces at the lateral walls acquire distinct values and do not exactly compensate one another [Figs. 2(d) and 2(e)]. Thus, the unbalanced shear force at the walls is compensated by the shear force at the base that tends to vanish with averaging over realizations [Fig. 2(f)].

We observe that during downward motion the normal forces on the sidewalls and the base are considerably larger than the weight of the column P_c (dashed lines in Fig. 2 represent $P_c \sim 2.3$ N). In contrast, in the upward cycle, the normal force on sidewalls is slightly lower than P_c. More importantly,

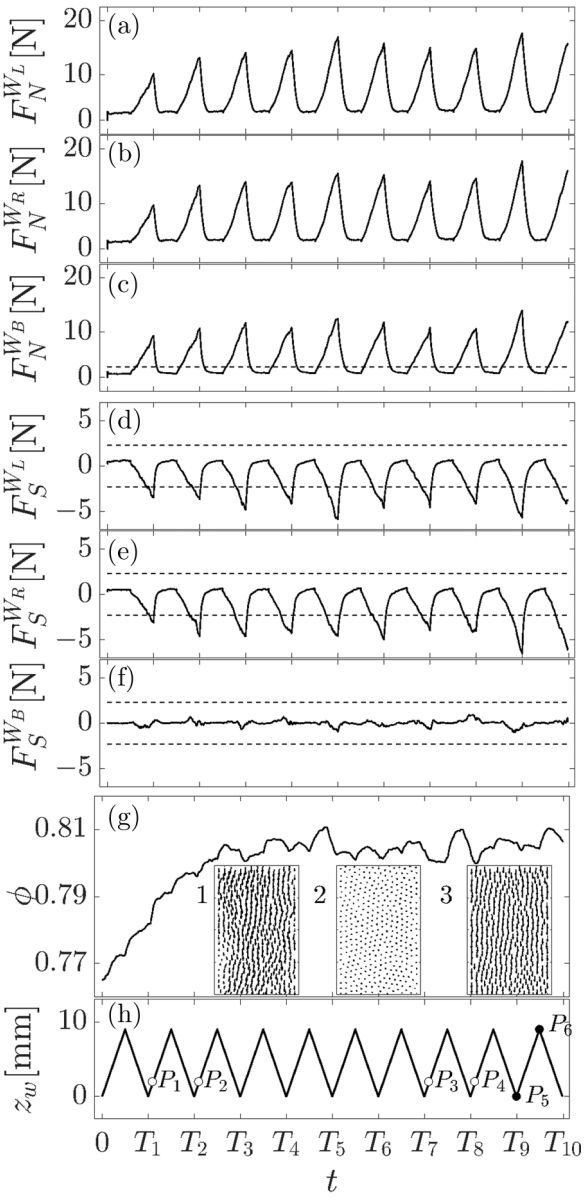

FIG. 2. Typical behavior of forces and packing, averaged over 20 realizations, as a function of time. Normal force on the sidewalls: left (a), right (b), and the base (c). Shear force on the sidewalls: left (d), right (e), and the base (f). The dashed lines indicate the weight of the column of grains $P_c \sim 2.3$ N. (g) The packing fraction ϕ. Insets: Relative grain displacement fields; 1: at walls position P_2 with respect to P_1; 2: at P_4 with respect to P_3; and 3: at P_6 with respect to P_5. Positions P_1–P_6 are indicated in (h). (h) Walls move following a triangular waveform: both sidewalls move upward and then downward in an alternate motion at a constant speed $v_w = 9$ mm/s. The horizontal axis is common to all graphs.

the normal force at the base is significantly lower than P_c, indicating the existence of a screening effect which reduces the pressure at the bottom of the column [Fig. 2(c)]. The shear force on the sidewalls rapidly reaches a plateau of about ∼0.5 N, which is approximately twice the weight of the column.

The relaxation of the system to a stationary state is better visualized in the packing fraction curve, ϕ, obtained by

averaging over 20 realizations [Fig. 2(g)]. In addition to a small modulation due to the cycling, a clear exponential relaxation is observed with the number of cycles. For these parameters, relaxation takes about three cycles. The steady state value of the packing fraction is $\phi \sim 0.805$ [corresponding to the average in time of ϕ at the plateau in Fig. 2(g)] and is slightly above the critical value of the jamming transition, obtained numerically in frictional disks $\phi_c \sim 0.795$ with $\mu \sim 0.8$ [12]. During the initial cycles, the packing fraction is smaller than the critical value, and the column of grains deforms plastically, i.e., showing irreversible changes in the position of particles within the cycle [see inset 1 in Fig. 2(g)]. However, at steady state, these irreversible trajectories are no longer observed, which suggests that the column is compressed, like an elastic material. Indeed, inset 2 in Fig. 2(g) shows that particles return to their initial positions after one cycle with little irreversible motion (inset 3 indicates the range of elastic deformation). Thus, jamming of the granular system prevents the relative sudden displacement usually associated with plastic events or irreversible movements. In the light of these observations, the sharp peaks in force, occurring at the point of maximum downward displacement, are the result of a jamming behavior.

A. Modification of the stress profile due to friction mobilization

In this section we study the evolution of the vertical stress profile, σ_{zz}, at the center of the column of grains as a function of the sidewall phase motion for $R_a \sim 3.2$ and $R_a \sim 9.6$ which correspond to small and large filling heights, respectively. σ_{zz} is obtained in the coarse graining framework [13,14] by averaging the corresponding component of the stress tensor along the x direction within a window of height $3d$ and width $6d$, centered at $x = 0$ [Fig. 1(a)]. The variation of stress with the vertical coordinate is obtained by averaging over the coarse graining window at successive positions along the vertical. For each wall position, further averaging is performed over several realizations of stress fields. Additionally, the effect of variation in the silo width σ_{zz} and the dependence of σ components on x are briefly mentioned.

1. Small filling height

During the upward motion of the sidewalls, presented in Fig. 3(a), a saturating profile is observed in σ_{zz} which resembles a Janssen-like profile, characterized by a negative curvature (curve A). Following the upward progression of the sidewalls, σ_{zz} stays in a Janssen-like profile until the sidewalls reach their maximum position at $z_w = 1d$. Then, the motion of the sidewalls is reversed and σ_{zz} changes form, from a saturating to a linear profile at the position $z_w \sim 0.78d$ (curve B). This indicates that the entire system has reached a hydrostatic regime and as a result only a small fraction of the friction is mobilized along the walls. Beyond this transition point, the σ_{zz} curvature sign becomes positive, which results in exponentially growing profiles (curve C). This indicates a reversal of the friction force and is directed downward. It is worth mentioning that σ_{zz} profiles become steeper as the sidewalls move towards the base. The state of saturating profiles is characterized by the length l, which is obtained by fitting Janssen's solution (2) to σ_{zz} values. We observe that l fluctuates around an average value $\langle l \rangle \sim 0.135$ mm during the upward motion of

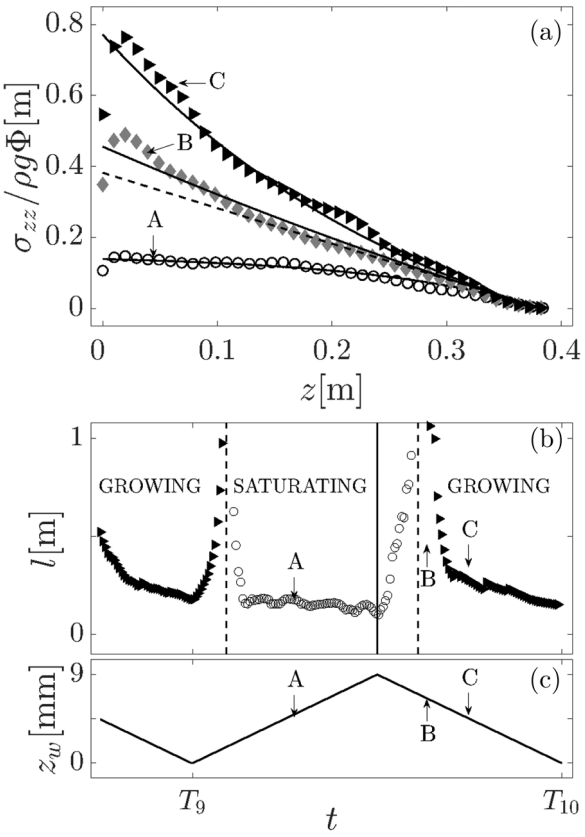

FIG. 3. (a) Average vertical stress profiles σ_{zz} obtained at the center of the column of grains, normalized to $\rho g \phi$ which correspond to three different positions of the sidewalls $z_w \sim 0.60d$ (curve A), $z_w \sim 0.75d$ (curve B), and $z_w \sim 0.60d$ (curve C), and their respective fitted curves (continuous lines), calculated from Janssen's analysis. The dashed line with slope $\rho g \phi$ represents the stress profile in the hydrostatic regime. (b) The characteristic length l obtained by fitting Janssen's solution to the vertical normalized stress profiles. The vertical dashed lines indicate the point of transition from exponentially growing to saturating regime and vice versa. (c) The relative position of the sidewalls z_w with respect to the position of the base after ninth cycle. (b) and (c) share the horizontal axis.

sidewalls [Fig. 3(b)]. Once the motion of sidewalls is reversed, a saturating profile is still observed. However, l starts to rapidly increase. This strong variation in l is due to significant changes in the mobilization of frictional forces. When sidewalls approach $z_w \sim 0.78d$, the magnitude of l grows almost exponentially and, as previously mentioned, σ_{zz} tends to a linear profile, indicating transition from a granulate to hydrostatic regime. Conversely, the state of exponentially growing profiles are characterized by a similar length l which is obtained using

$$\sigma_{zz}(z) = \rho g \phi l \left[\exp\left(\frac{z_0 - z}{l} \right) - 1 \right], \tag{3}$$

as a fitting function, which in turn is derived from Eq. (2) by inverting the sign of friction. Take note that in engineering literature, the inversion of the friction sign in Janssen's profile is observed when the granular column expands after filling, or when the walls of the container are contracted by an external agent. This situation is referred to as a *true passive regime* [15]. Although the true passive regime replicates the

profiles observed in this investigation, the physical origin of this profile is markedly different. It is observed that l rapidly decreases immediately after exponential growth of the σ_{zz} profile. This decrease in l is nearly exponential, reaching an asymptotic value of ~ 0.2 m. It is worth mentioning that this is also observed during the reverse transition, from exponentially growing to a saturating profile, and similar features are obtained. Indeed, when the sidewalls' motion is reversed from downward to upward, l also increases almost exponentially, and σ_{zz} tends to a linear profile. Hence, this transition is also marked by hydrostatic behavior in the column of grains. It should also be noted that l should be formally infinite at the transition point. However, experimentally it is difficult to conclude the exact dependence of l to the displacement of the sidewalls, because the variation occurs over a limited range of z_w.

It is apparent from Fig. 3 that the full transition between these two states of opposite mobilization requires a small wall displacement, noticeable by comparison of Figs. 3(b) and 3(c). This characteristic distance, measured as the distance between the end of the state characterized by exponentially growing profiles (coincident with the wall motion inversion) to the beginning of the plateau of saturating σ_{zz} [Fig. 3(b)], is about $1/3$ of a particle diameter. This displacement corresponds roughly to the typical sliding distance of grains necessary to fully mobilize the frictional force at the walls. Once the transition is achieved the system remains in one of these states until the wall motion is again inverted.

A time shift is observed between forces and peaks in l. Peaks in forces occur only in downward cycles, and are located at the minimum displacement of sidewalls $z_w \approx 0$, whereas the maximum compression is applied to the column of grains [Figs. 2(a)–2(e)]. On the other hand, l shows maximum values at locations $z_w \sim 0.19d$ in the upward cycle, and $z_w \sim 0.78d$ in the downward cycle. These values of z_w correspond to the necessary displacement required to minimize friction at the walls, allowing the column to transit to a hydrostatic state. In the next section we explore the effects of increasing the silo filling. It is shown that frictional forces are not homogeneously mobilized along sidewalls, which results in a strong modification of σ_{zz} profiles, in both upward and downward cycles.

2. *Large filling height*

In this section we study how the transition, observed in the previous section, is modified for by increasing of the filling height to $h \sim 1.2$ m, which changes the aspect ratio to $R_a \sim 9.6$. The observed compaction and decompaction of the column of grains is relevant along the z axis in terms of quantity. Due to the minor compaction and decompaction, they are characterized through a relative packing, defined as $\Psi = (\phi - \phi_{\text{ref}})/\phi_{\text{ref}} \times 100$, where ϕ is the local packing fraction (the ratio of the area occupied by grains to the total area of the control surface) and ϕ_{ref} is a packing reference, for instance from that observed in the Janssen's state. Here it is noted that all quantities are defined in the approximation of coarse graining, which varies along the grains column and is obtained from the numeric, using a window of area $D \times 3d$ centered at $x = 0$, which slides by a small fraction of d to give the behavior along the z axis. Similar to the behavior taking place in the low filling height scenario, observation of particle trajectories (not shown) during the initial cycles indicate that Ψ is predominantly modified by irreversible or plastic displacement of the grains, and to a lesser extent by the elastic response of the grains themselves. On the contrary, after a few steady state cycles, the absence of irreversible trajectories indicates that variation of Ψ in a cycle is almost entirely dominated by the elastic compression of the grains. It is important to note that, for wall displacement in this simulation, Janssen's state is easily reached for upward motion, which provides a well-defined reference state. Starting at the maximum high of the walls, it is observed that Ψ increases more rapidly at the bottom of the silo, as the sidewalls move downward, and exponentially decays with z [see Fig. 4(a) whose reference is the Janssen's state at the highest position of the walls, $\phi_{\text{ref}} = \phi(z_w = 1d)$].

The horizontal to vertical stress ratio $\kappa = \sigma_{xx}/\sigma_{zz}$ shows a slight variation with the vertical coordinate z and wall displacement [Fig. 4(b)], which can be considered constant in a first approximation, $\kappa \sim 1$. Friction $\mu = (\sigma_{xz}/\sigma_{xx})$ at the sidewalls shows a sign reversal, which gradually propagates from the bottom of the silo, resembling a moving front of sign reversal [Fig. 4(c)], see Supplemental Material [16]. The maximum penetration of this front approximately corresponds with the location where Ψ starts to increase, [compare Figs. 4(a) and 4(c)]. Beyond this length, both μ and Ψ remain almost unchanged, indicating little effect of the sidewalls' motion in this region of the silo.

Initiating at the highest position of the walls, at a Janssen's state, the downward motion of the walls leads to increasing stress σ_{zz} at the base of the pile, which causes the profile to gradually invert its curvature [Fig. 4(d)]. The stress profile exponentially increases close to the base of the pile due to the inversion of friction mobilization. However, a persistent Janssen-like regime occurs at the uppermost part of the column of grains. Hence, the downward displacement of the sidewalls induces the coexistence of two regions with opposite friction mobilizations. In turn, this is responsible for the combination of Janssen-like and exponentially growing stress profiles in the grain column.

When the motion of the sidewalls is reversed, from the lowermost position, the Ψ gradually decreases from the observed maximum value. This decrease is propagated along the pile and decays exponentially with height [Fig. 5(a)]. Similar to the downward motion, κ varies slightly around (1) and may be considered constant [Fig. 5(b)]. In contrast to the observations during downward movement, the two regions of opposite friction mobilization retract with the sidewalls' motion. However, the limiting zone is not retracted as a front, and instead it moves as a block. As a consequence, the two regimes in the stress profile rapidly transit to a single Janssen-like profile, requiring only minor displacement of the sidewalls, equivalent to a small fraction of the particles' diameter [Fig. 5(d)].

3. *Effect of silo width on σ_{zz}*

This section briefly analyzes the effect of the silo width on the σ_{zz} profile. If the filling height is maintained at $h \sim 1.2m$, and the silo width is increased to $1.5D$ ($R_a \sim 6.4$), during the

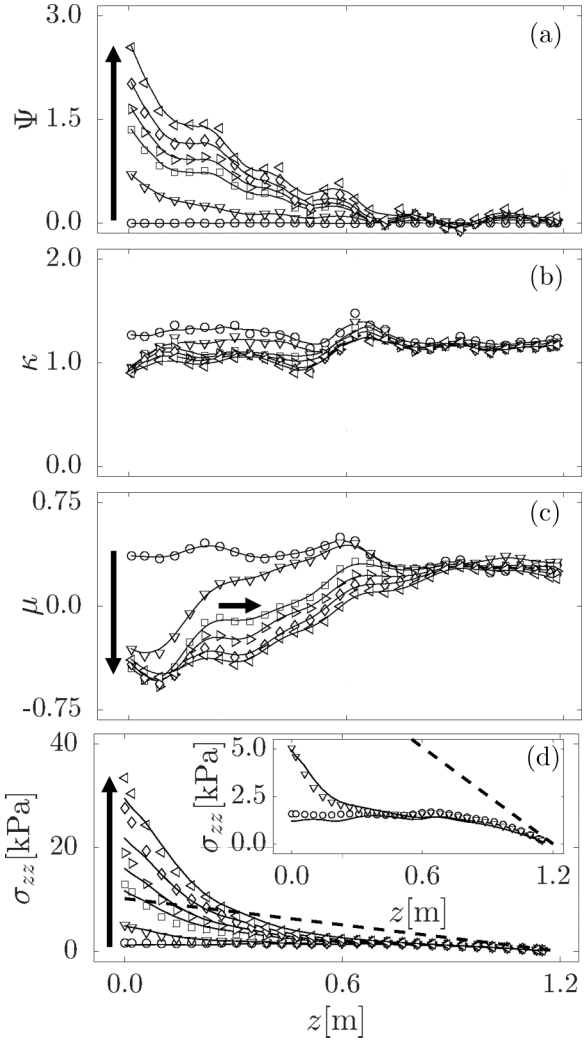

FIG. 4. Characteristic curves for a large filling height, downward motion case. (a) $\Psi = (\phi - \phi_{\text{ref}})/\phi_{\text{ref}} \times 100$; ϕ_{ref} is the reference packing fraction at $z_w = 9$ mm (the Janssen's state). (b) $\kappa = \sigma_{xx}/\sigma_{zz}$. (c) Friction μ at the sidewalls and (d) σ_{zz}. Continuous curves in (a), (b), and (c) are guiding curves and do not correspond to a fit. In (d) the continuous curves are obtained by integrating Eq. (4) using μ as input. (Inset) Zoom of curves for very small displacement respect to the reference state. The dashed line represents the hydrostatic limit. The symbols indicate the height of the sidewalls: $z_w \sim 9$ mm (◯), $z_w \sim 7$ mm (▽), $z_w \sim 5$ mm (□), $z_w \sim 3$ mm (▷), $z_w \sim 2$ mm (◇), and $z_w \sim 0$ mm (◁).The horizontal axis is common to all graphs. Arrows indicate profiles for decreasing positions on the wall.

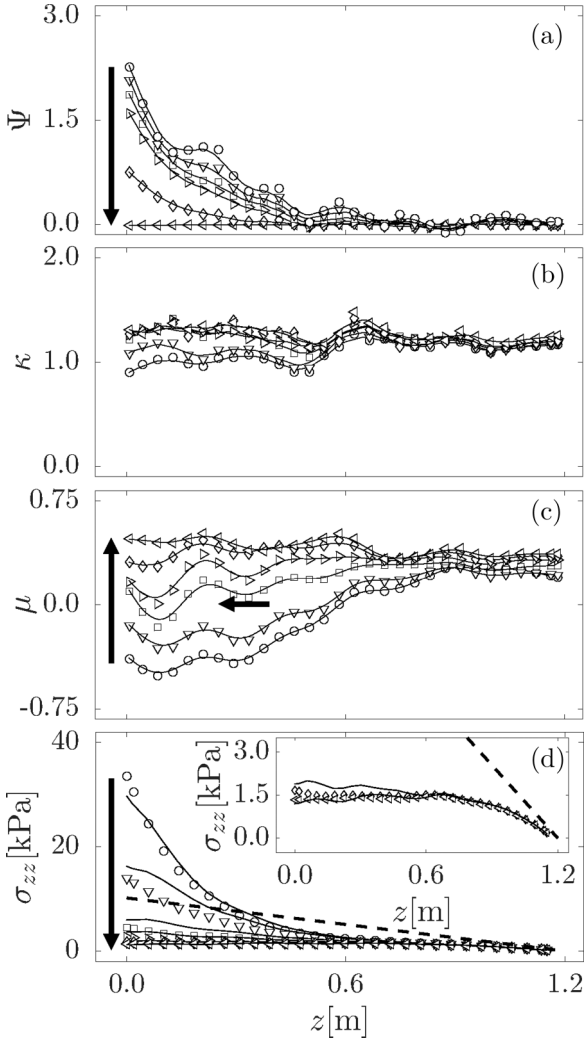

FIG. 5. Characteristic curves for a large filling height, upward motion case. (a) $\Psi = (\phi - \phi_{\text{ref}})/\phi_{\text{ref}} \times 100$; ϕ_{ref} is the reference packing fraction at $z_w \sim 9$ mm (Janssen's state). (b) $\kappa = \sigma_{xx}/\sigma_{zz}$. (c) Friction μ at the sidewalls and (d) σ_{zz}. Continuous curves in (a), (b), and (c) are guiding curves and do not correspond to a fit. In (d) the continuous curves are obtained by integrating Eq. (4) using μ as an input. (Inset) Zoom of curves for very small displacement respect to the reference state. The dashed line represents the hydrostatic limit. The symbols indicate the relative displacement of the sidewalls: $z_w \sim 0$ mm (◯), $z_w \sim 2$ mm (▽), $z_w \sim 5$ mm (□), $z_w \sim 6$ mm (▷), $z_w \sim 7$ mm (◇), and $z_w \sim 9$ mm (◁). The horizontal axis is common to all graphs. Arrows indicate profiles for increasing positions on the wall.

loading cycle σ_{zz} shows characteristics similar to those found in the scenario of large filling. Specifically, the scenario maintains the coexistence of exponentially growing and saturating profiles. However, in Fig. 6(b) the plateau region decreases and both profiles are approached (curve □). If the number of particles is kept constant ($N = 2200$), and the width is increased to $4D$ ($R_a \sim 0.6$), the system maintains a permanent hydrostatic regime with a linear profile, regardless of the direction of motion of the sidewalls [curves ◯ in Figs. 6(a) and 6(b)]. For comparison, the small filling case $R_a \sim 3.2$ is shown [curve ▷ in Fig. 6(b)]. By contrast, during the unloading cycles the stress profile shows a Janssen-like regime for any $R_a \geqslant 3.2$, and a hydrostatic regime for $R_a \sim 0.6$. In summary, independent of the motion of sidewalls, the system is in a pure hydrostatic regime for $R_a < 1$, and a Janssen-like regime for $R_a > 1$ in the unloading cycle. Otherwise, we observe that during the loading cycle a transition from two coexistent profiles to a single profile occurs, at approximately $R_a \sim 3$.

4. Dependence of σ on x

The average σ components as a function of x are investigated in the following. It is observed that σ_{xx} is independent of x, whereas its magnitude decreases with z_w [Fig. 7(a)].

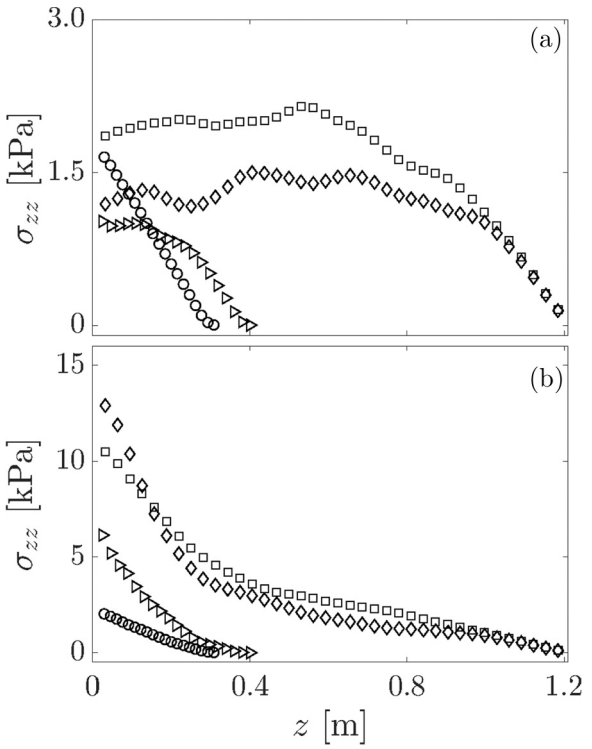

FIG. 6. Effect of the aspect ratio on σ_{zz}: (a) in the unloading and (b) loading cycles. $R_a \sim 0.6$ (◯), $R_a \sim 3.2$ (▷), $R_a \sim 6.4$ (□), and $R_a \sim 9.6$ (◇). The z axis is shared by (a) and (b).

In turn, σ_{zz} is symmetric with respect to the column center and decreases from the maximum value towards the sidewalls. The maximum value of σ_{zz} increases when sidewalls move downward [Fig. 7(b)]. Conversely, σ_{xz} shows a monotonic behavior, which is approximately linear with x [Fig. 7(c)]. Note that, the slope of σ_{xz} depends on the friction force. If the friction is oriented positively in z, the slope of σ_{xz} is positive, which corresponds to an upward motion of sidewalls. In contrast, when sidewalls move downward, the friction sign reverses to a negative orientation in z, resulting in a negative slope of σ_{xz}. During transition, $\sigma_{xz} \sim 0$, indicating a minimal frictional force in the hydrostatic state observed in the σ_{zz} profile.

B. Janssen's equation with variable friction mobilization

In order to explain the complexity of the stress profile the following scenario is utilized: the system is placed under a general state of nonhomogeneous friction, either total or partially mobilized, by extending Janssen's analysis. The Janssen's equation is a force equilibrium equation, derived for fully mobilized frictional forces excluding the dependence of friction on the loading history. Therefore, in order to account for partial mobilization, it is considered that a particular state of nonhomogeneous friction, obtained after the sidewalls are displaced relative to the base, is fully characterized by a generalized frictional coefficient $\mu(z)$. $\mu(z)$ is simply defined as the value of the shear- to normal-force ratio at the sidewalls, $\mu(z) = F_S(z)/F_N(z)$. Subsequently, the force

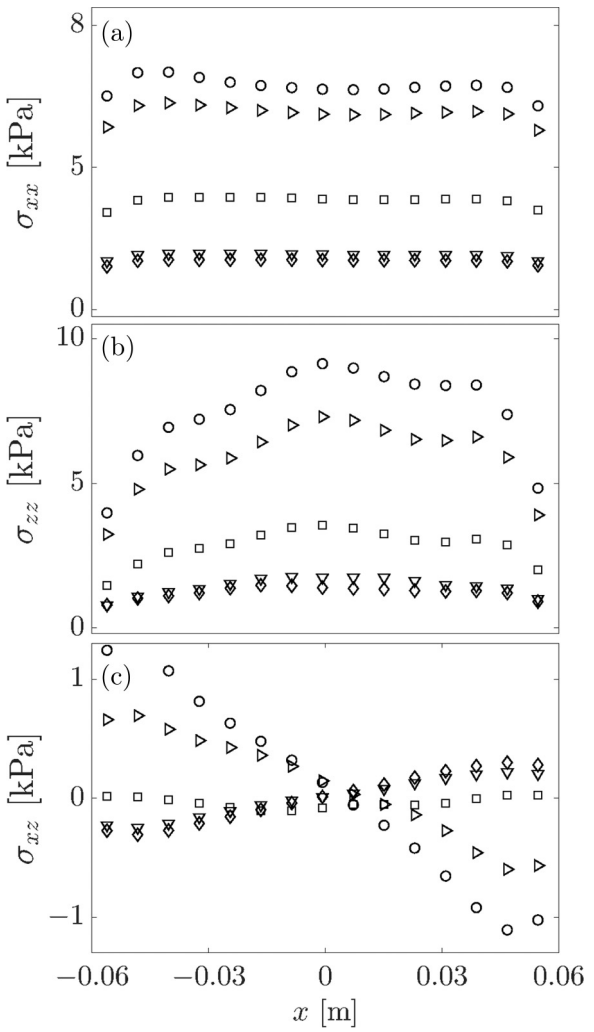

FIG. 7. σ components as a function of x for different positions of the sidewalls and $R_a \sim 9.6$. (a) σ_{xx}, (b) σ_{zz}, and (c) σ_{xz}. $z_w \sim 0,0.2,0.6,0.8,1$ (◯, ▷, □, ▽, ◇). (a), (b), and (c) share the x axis.

equilibrium Eq. (1) reads

$$-\frac{d\sigma_{zz}}{dz} + \frac{\kappa\mu(z)}{D}\sigma_{zz} = \rho g\phi. \tag{4}$$

For a given function $\mu(z)$ this equation can be formally integrated using the integrating factor method. Then, assuming the initial condition in the upper section of the column of grains $\sigma_{zz}(L) = 0$, an analytic expression is obtained for the solution of Eq. (4) in terms of friction $\mu(z)$, which can be written as

$$\sigma_{zz} = -\left[\rho g\phi \int_L^z \exp\left(-\frac{\kappa}{D}\int_L^{z'} \mu(z'')dz''\right)dz'\right] \times \exp\left(\frac{\kappa}{D}\int_L^z \mu(z')dz'\right). \tag{5}$$

In general, the analytic expression of $\mu(z)$ is unknown, due to its strong dependence on the loading history. Therefore, effort is focused to verify the consistence of Eq. (5). The following procedure is implemented: primarily, directly obtain the frictional coefficient from numerical simulations by averaging over realizations as $\langle\mu(z)\rangle = \langle F_S(z)/F_N(z)\rangle$, then compare the

σ_{zz} profiles obtained from simulations with solutions of Eq. (4) obtained numerically using the fourth-order Runge-Kutta method and the corresponding $\langle\mu(z)\rangle$ as an input. The step size of the integration is adapted to match the points of known values of $\langle\mu(z)\rangle$. The extra half-step-size values, required by the Runge-Kutta algorithm, are obtained by interpolation. It is observed that for each state of nonhomogeneous friction $\langle\mu(z)\rangle$, the main features presented in normalized σ_{zz} profiles are qualitatively captured by solutions of Eq. (4) [Figs. 4(d) and 5(d)]. In particular, these solutions contain the coexistence of saturating and exponentially growing profiles obtained from simulations. Thus, the generalization of Janssen's analysis reproduces the main features of the vertical stress profiles σ_{zz}, capturing the coexistence of exponentially growing and saturating regimes, observed where friction is nonhomogeneous and partially mobilized.

Despite the results given above, the issue is still open regarding how the history dependence of partially mobilized friction can be included in mathematical analysis. In the following, small changes in friction mobilization are accounted for by assuming that the friction force at the wall depends on the history through a displacement w, defined as the relative vertical displacement between grains and sidewalls. For nonhomogeneous mobilization, it is assumed that w depends on the vertical position along the wall, $w(z)$. In addition, this approach requires the well-known friction mobilization state of the column, used as a reference for changes in friction [2]. In this case, the Janssen-like state, where the effective friction is fully mobilized, provides a suitable reference state. Similar to what is observed in the case of the small filling height, the absence of irreversible particle trajectories (in the steady state of the large column of grains), indicates that the stress distribution can be described using linear elasticity, as in [2]. Specifically, at steady state, variation in the columns' relative volume along the vertical is predominantly modified by the elastic deformation of the grains themselves, and the contribution from packing fraction is negligible. Subsequently, the stress tensor components are replaced with the corresponding expressions in terms of the strain tensor components, similarly to Evesque and de Gennes [2]. Due to the lateral confinement of the column, the horizontal strain is $\varepsilon_{xx} = 0$, which leads to

$$\sigma_{zz} = \frac{E_C}{(1+\nu_C)(1-\nu_C)}\varepsilon_{zz}, \tag{6}$$

$$\sigma_{xx} = \frac{E_C \nu_C}{(1+\nu_C)(1-\nu_C)}\varepsilon_{zz}, \tag{7}$$

where E_C and ν_C are the effective Young's modulus and Poisson's ratio of the granular column. Subsequently, we assume that the transition from the Janssen's state to the exponentially growing regime can be described by an effective friction coefficient which varies exponentially from $\mu = \mu_0$ (Janssen) to $\mu = -\mu_0$ (exponentially growing). This is

$$\mu(w) = \mu_0\left[-1 + 2\exp\left(-\frac{w}{\lambda_\mu}\right)\right], \tag{8}$$

where λ_μ is the characteristic relative displacement required to reverse the sign of the partially mobilized friction. This characteristic displacement is obtained from numerical results by following the variation of the ratio of the tangential force to the normal force with z_w at the base of the column. We obtained $\lambda_\mu \sim 0.9$ mm $\approx 0.1d$. Considering the assumptions above, Eq. (4) is transformed into

$$-\frac{d\varepsilon_{zz}}{dz} + \nu_C\frac{\mu(w)}{D}\varepsilon_{zz} = \rho g\phi\frac{(1+\nu_C)(1-\nu_C)}{E_C}, \tag{9}$$

where Janssen's parameter κ (in the elastic approximation) is identified as $\kappa \equiv \sigma_{xx}/\sigma_{zz} = \nu_C$ [2]. We then consider a small friction mobilization with respect to the reference state, $w \ll \lambda_\mu$, which leads to $\mu(w) \sim \mu_0(1 - 2w/\lambda_\mu)$. Finally, in order to derive a useful equation for w, the total displacement of grains with respect to the wall must be related to the elastic strain. At the reference state, the layer already has some strain; we thus write, $\varepsilon_{zz} \approx \varepsilon_J + \frac{dw}{dz}$, where ε_J is Janssen's strain. Introducing in Eq. (9) and preserving only linear terms, this ultimately gives,

$$-\frac{d^2w}{dz^2} + \nu_C\frac{\mu_0}{D}\frac{dw}{dz} - 2\varepsilon_J\nu_C\frac{\mu_0}{D}\frac{w}{\lambda_\mu} = 0. \tag{10}$$

Inspection of Eq. (10) reveals two characteristic lengths: a penetration length, $l_\Psi = \frac{D}{\mu_0}(\frac{1}{\nu_C})$, and a typical wavelength of profile oscillation, $\lambda = 2\pi\sqrt{\frac{D\lambda_\mu}{2\nu_C\mu_0\varepsilon_J}}$. Although Eq. (10) can be solved with appropriate boundary conditions, here it is limited to a qualitative comparison of these scales with the features of simulated profiles. First, it is established that the variation of ϕ with respect to the Janssen's state is simply $\Psi \approx \frac{dw}{dz}$. An estimation of penetration length from the curves in Fig. 4(a) gives $l_\Psi \sim 0.32$ m, which is approximately 2.5 times the column width. Second, considering this, the estimated Janssen parameter $\kappa = D/(l_\Psi\mu_0) \approx 0.97$, which agrees with the observed mean value of the curves in Fig. 4(b). Thus, we conclude that the vertical stress profile of a granular column for partial mobilization of friction, induced by the vertical motion of the sidewalls, can be qualitatively captured by a modified Janssen's equation including a nonhomogeneous friction coefficient. According to a first approximation, this effective friction coefficient depends solely on the sliding distance of grains at the walls. The effect of the second length scale, λ, originating from column elasticity, is unclear. Our estimate indicates that this length is greater than the silo height and therefore not relevant to this case.

IV. CONCLUSIONS

This investigation presents the response of packing, friction mobilization, and the vertical stress profile of a 2D column of grains, caused by the triangular vertical motion of the sidewalls. After a few cycles, homogeneous bidisperse granulates reach a stationary regime which is characterized by a jamming state, where variations in packing are dominated by the elastic compression of grains. It should be noted that after compression elastic energy is accumulated in the granular system because of the low value of Young's modulus of grains. This elasticity controls the required scale of displacement to mobilize friction force. In contrast, if grains are replaced by extremely rigid particles, friction mobilization would have a more sudden response to the motion of the walls. The ratio of the maximum shear force to the maximum normal

force at sidewalls is lower than the maximum attainable friction, indicating that frequently the friction force is not fully mobilized. The system shows distinctive regimes for vertical stresses which are controlled through the inversion of frictional forces induced by the vertical motion of sidewalls. In general, the downward displacement of sidewalls results in an exponential increase of packing at the base and within the surrounding area, and a friction force inversion. As a consequence, the sign of local curvature of the vertical stress reverses to negative, which results in a local exponential growth. Conversely, if the motion of sidewalls is reversed from downward to upward, the packing is decreased and the friction force re-inverts, which results in a Janssen-like profile.

More specifically, the penetration length of the reverse friction profile depends mainly on the aspect ratio of the system. For wide silos ($R_a \sim 0.6$), friction is not significant and the system remains in a hydrostatic regime characterized by a linear stress profile which is independent to the direction of the sidewalls motion. By increasing $R_a \sim 3.2$, friction force effects become significant. The penetration length is slightly longer than the filling height, which results in two different regimes: a Janssen-like regime induced by the upward motion of sidewalls, characterized by a saturating stress profile, and a loaded regime induced by the downward motion of sidewalls, characterized by an exponentially growing profile. The transition between these two regimes is marked by a hydrostatic state characterized by a linear profile. If the aspect ratio is increased to $R_a \sim 9.6$ the system exhibits a more complex behavior. In this case, the penetration length is much less than the filling height, which allows for the development of two coexisting zones of partially mobilized friction force, with an opposite sign. The stress profile can show two distinctive regimes: a Janssen-like regime for upward movement of the sidewalls, and a combination of loaded and Janssen-like regimes for downward movement. In the latter, the vertical stress shows the coexistence of an exponentially growing profile near the base of the pile, and a Janssen-like profile close to the top of the granulate. These profiles are connected through a plateau region, which varies in size depending on the aspect ratio of the system. A generalized version of Janssen's equation, which includes a general state of nonhomogeneous friction (either totally or partially mobilized) is necessary for the reproduction of the coexisting exponentially growing and saturating profiles, obtained when the penetration length is less than the filling height.

ACKNOWLEDGMENTS

F.V. acknowledges funding support from Conicyt (Chile) through Fondecyt No. 1120615. F.M. is very grateful to the NICOP program, from the USA Navy for financial support.

[1] H. A. Janssen, Versuche über Getreidedruck in Silozellen, Z. Ver. Dt. Ing. **39**, 1045 (1895); see also M. Sperl, Experiments on corn pressure in silo cells, Translation and comment of Janssens paper from 1895, Gran. Matter **8**, 59 (2006).

[2] P. Evesque and P.-G. de Gennes, Sur la statique des silos, C. R. Acad. Sci. Paris, Série II b **326**, 761 (1998).

[3] L. Vanel, Ph. Claudin, J.-Ph. Bouchaud, M. E. Cates, E. Clément, and J. P. Wittmer, Stresses in Silos: Comparison Between Theoretical Models and New Experiments, Phys. Rev. Lett. **84**, 1439 (2000).

[4] G. Ovarlez, C. Fond, and E. Clément, Overshoot effect in the Janssen granular column: A crucial test for granular mechanics, Phys. Rev. E **67**, 060302 (2003).

[5] Y. Bertho, F. Giorgiutti-Dauphiné, and J.-P. Hulin, Dynamical Janssen Effect on Granular Packing with Moving Walls, Phys. Rev. Lett. **90**, 144301 (2003).

[6] J. W. Landry and G. S. Grest, Granular packings with moving sidewalls, Phys. Rev. E **69**, 031303 (2004).

[7] V. Šmilauer, E. Catalano, B. Chareyre, S. Dorofenko, J. Duriez, A. Gladky, J. Kozicki, C. Modenese, L. Scholtès, L. Sibille, J. Stránský, and K. Thoeni, Yade Documentation, The Yade Project, 1st ed., 2010, http://yade-dem.org/doc/.

[8] PFC3D (particle flow code in 3D) theory and background manual, version 3.0, Itasca Consulting Group, 2000.

[9] V. Šmilauer and B. Chareyre, Yade DEM formulation, in Yade Documentation, edited by V. Šmilauer, The Yade Project, 1st ed., 2010, http://yade-dem.org/doc/.

[10] J. W. Landry, G. S. Grest, and S. J. Plimpton, Discrete element simulations of stress distribution in silos: crossover from two to three dimensions, Powder Technol. **139**, 233 (2004).

[11] J. W. Landry, G. S. Grest, L. E. Silbert, and S. J. Plimpton, Confined granular packings: Structure, stress and forces, Phys. Rev. E **67**, 041303 (2003).

[12] L. E. Silbert, Jamming of frictional spheres and random loose packing, Soft Matter **6**, 2918 (2010).

[13] B. J. Glassier and I. Goldhirsch, Scale dependence, correlations, and fluctuations of stresses in rapid granular flows, Phys. Fluids **13**, 407 (2001).

[14] C. Goldenberg, A. Tanguy, and J.-L. Barrat, Particle displacements in the elastic deformation of amorphous materials: local fluctuations *vs.* non-affine field, Europhys. Lett. **80**, 16003 (2007).

[15] R. M. Nedderman, *Static and Kinematic of Granular Materials* (Cambridge University Press, Cambridge, 1992).

[16] See Supplemental Material at http://link.aps.org/supplemental/10.1103/PhysRevE.94.022906 for evolution over time of the granular column, and σ_{zz} and μ profiles.